Computational Materials Science 49 (2010) S322–S325

Contents lists available at ScienceDirect

Computational Materials Science

journal homepage: www.elsevier.com/locate/commatsci

Some theoretical results on semiconductor spherical quantum dots

B. Billaud [a,b], T.-T. Truong [b,*]

[a] Laboratoire de Physique Théorique et Hautes Energies (LPTHE), CNRS UMR 7589, Université Pierre et Marie Curie (Paris VI), 4, place Jussieu, F-75252 Paris Cedex 05, France
[b] Laboratoire de Physique Théorique et Modélisation (LPTM), CNRS UMR 8089, Université de Cergy-Pontoise, 2, avenue Adolphe Chauvin, F-95302 Cergy-Pontoise Cedex, France

ARTICLE INFO

Article history:
Received 9 October 2009
Accepted 12 April 2010
Available online 5 May 2010

Keywords:
Spherical quantum dot
Semiconductor
Stark effect
Lamb shift
Purcell effect

ABSTRACT

We use an improved version of the standard effective mass approximation model to describe quantum effects in nanometric semiconductor quantum dots (QDs). This allows analytic computation of relevant quantities to a very large extent. We obtain, as a function of the QD radius, in precise domains of validity, the QD excitonic ground state energy and its Stark and Lamb shifts. Finally, the Purcell effect in QDs is shown to lead to potential QD-LASER emitting in the range of visible light.

1. Introduction

As semiconducting quantum dots (QDs) display standard atomic physics properties, they may be thought as giant artificial atoms, with adjustable quantized energy spectra through their sizes and shapes. They are of interest in a wide range of research areas [1–5]. In such structures, Quantum Size Effects (QSE) are characterized by a blue-shift in the semiconductor optical spectrum, due to the increase of the charge carrier confinement energy. Results on QSE in low-dimensional semiconductor structures and modern approaches to this problem are discussed in [6,7]. In this paper, the QD problem is dealt within a modified effective mass approximation (EMA) model, to which a pseudo-potential is added (*cf.* Section 2). This partially removes the over-estimation of the electron–hole pair confinement energy for small QDs, and allows the analytic determination of the Kayanuma function $\eta(\lambda)$ [8].

The physics of QDs, particularly in regard to the QD interaction with an external field, is very attractive. It gives rise to Quantum-Confinement Stark Effects (QCSE) [9,10], which manifest themselves through a red-shift of exciton photoluminescence [11]. In Section 3, we use the EMA model to obtain analytic criterions on the QD radius and the applied electric field amplitude, as a result of the interplay between electron–hole Coulomb interaction and an additional polarization energy [12]. When the electromagnetic field is quantized, an energy level Lamb shift occurs [13,14]. While it is a continual subject of research [15,16], it seems to be unknown for QDs. In Section 4, we use the EMA framework to uncover an observable negative Lamb shift for the electron–hole pair ground state, in judiciously chosen QDs. In Section 5, the Purcell effect, a test bed for many applications [17–19], is studied for QDs. A condition for its occurrence, despite the action of unfavorable Rabi oscillations, is derived. This opens the way for a visible light QD-LASER, driven by a Purcell effect.

2. Quantum Size Effects

In a standard EMA model, an electron and a hole, of effective masses $m^*_{e,h}$, behave as free particles in a spherical infinite potential well $V(\mathbf{r}_{e,h})$. Their Coulomb interaction $-\frac{e^2}{\kappa r_{eh}}$ is treated by a variational procedure. To handle the interplay between confinement energy (scaling as $\propto R^{-2}$), and Coulomb potential (scaling as $\propto R^{-1}$), two regimes are singled out by the values of the ratio of the QD radius R to the bulk Mott–Wannier exciton Bohr radius a^* [8]. Here, as far as Stark, Lamb or Purcell effects are concerned, the so-called weak field limit, by which the charge carriers cannot overstep the real confining potential by tunneling, is assumed.

In a strong confinement regime, where $R \lesssim 2a^*$, the electron–hole relative motion is affected by the infinite potential well, such that the electron–hole pair stays quasi-uncorrelated. To exhibit the excitonic behavior of the electron–hole pair, both electron and hole, individually confined and being in their ground state, the following trial function $\phi(\mathbf{r}_e, \mathbf{r}_h) \propto e^{-\frac{\sigma' eh}{2a^*}}$, of parameter σ, is to be used. The electron–hole pair ground state energy $E^{strong}_{eh} = E_{eh} - 1.786\frac{e^2}{\kappa R} - 0.248E^*$, given in [8], is retrieved up to $\left(\frac{R}{a^*}\right)^2$ order, μ being the electron–hole pair reduced mass, $E_{eh} = \frac{\pi^2}{2\mu R^2}$ its ground state confinement energy, and E^* the excitonic Rydberg energy.

* Corresponding author.
E-mail address: truong@u-cergy.fr (T.-T. Truong).

0927-0256/$ - see front matter © 2010 Elsevier B.V. All rights reserved.
doi:10.1016/j.commatsci.2010.04.010

In the weak confinement regime, where $R \gtrsim 4a^*$, the exciton behaves as a quasi-particle of mass $M = m_e^* + m_h^*$. Then, the leading contribution to its ground state energy is $-E^*$, while its total translational motion is $\frac{\pi^2}{2MR^2}$. To improve the accuracy of the exciton ground state energy $-E^* + \frac{\pi^2}{2MR^2}$, a phenomenological function $\eta(\lambda)$ of the mass ratio $\lambda = \frac{m_h^*}{m_e^*}$ was introduced in [8]. The exciton is thought as a rigid sphere of radius $\eta(\lambda)a^*$, and its center-of-mass cannot reach the infinite potential well boundary unless the electron–hole relative motion undergoes a strong deformation [8]. Thus, adding a ground state plane wave in the center-of-mass coordinates to the trial function $\phi(\mathbf{r}_e, \mathbf{r}_h)$, we obtain, up to $\left(\frac{a^*}{R}\right)^3$ order, $E_{eh}^{weak} = -E^* + \frac{\pi^2}{6\mu R^2} + \frac{\pi^2}{2M(R-\eta(\lambda)a^*)^2}$, where $\eta(\lambda) = 0.208\frac{(1+\lambda)^2}{\lambda}$. $\eta(\lambda)$ satisfies the electron–hole exchange symmetry, and Table 1 shows good agreement with computational results.

However, E_{eh}^{weak} has a further kinetic energy term $\frac{\pi^2}{6\mu R^2}$ in the relative coordinates [8]. As the virial theorem should be satisfied in these coordinates, this energy is already contained in the Rydberg energy. To remove this contribution, we propose to add the pseudo-potential $W(\mathbf{r}_{eh}) = -\frac{32\pi^2}{9}E^*\frac{r_{eh}^2}{R^2}e^{-2\frac{r_{eh}}{a^*}}$.[1] This pseudo-potential also decreases the exciton energy by $\approx -19.9E^*$ in the strong confinement regime. Fig. 1 shows that the excitonic energy computed with $W(\mathbf{r}_{eh})$ shows a better fit to experimental results for $2R \lesssim a^*$. The divergence for very small QD size still persists as a consequence of the infinite potential well assumption [20]. To improve predictive results in this region, energy expansions may be carried out to a few more orders. But, computations become so involved that the relevance of such an approach can be questioned.

3. Quantum-Confinement Stark Effects

An electric field $\mathbf{E}_d$, is applied along the z-axis of a cartesian coordinates system with its origin at the QD center. Even if the EMA model does not fully describe the QD behavior in the absence of electric field, it can be still used to study QCSE in the weak field limit but should include the dipolar interaction $W_{e\,h}(\mathbf{r}_{eh}) = \mathbf{E}_d \cdot \mathbf{d}_{eh}$, $\mathbf{d}_{eh}$ being the exciton dipole moment. The quantity eE_dR, where $E_d = |\mathbf{E}_d|$, is treated as a perturbation. Following [22], we use here the trial function $\phi(\mathbf{r}_e, \mathbf{r}_h)$, describing the electric field free electron–hole pair, but with electric field interaction factors $e^{\mp\frac{\sigma_{e,h}}{2}z_{e,h}}$ of parameters $\sigma_{e,h}$, to account for the spherical shape deformation along $\mathbf{E}_d$.

The Stark shift is determined, up to $\frac{R}{a^*}$ order, as $\Delta E_{Stark}^{strong} = -\Gamma M e^2 E_d^2 R^4\{1 + \Gamma_{eh}\frac{R}{a^*}\}$, where $\Gamma \approx 0.018$ and Γ_{eh} depends on the semiconductor. The first contribution is the sum of the Stark shifts undergone by the electron and hole ground states. The second contribution expresses the remnant of electron–hole pair states as exciton bound states. As the inside semiconducting QD dielectric constant ε is larger than the outside insulating matrix one, the polarization energy $P(\mathbf{r}_e, \mathbf{r}_h)$ introduced in [23] is also considered, and its relative role *vs.* the Coulomb potential explored. Explicit analytical expressions for any Stark effect quantity, pertaining either to the polarization energy or to its combined effect with Coulomb potential, are given in [12], and successfully confronted with computational data [10].

For $CdS_{0.12}Se_{0.88}$ microcrystals, the strong confinement regime and the weak field limit condition are fulfilled for $E_d \approx 12.5\ kV\,cm^{-1}$ and $R \lesssim 30$ Å, if Coulomb interaction and polarization energy are taken to account. When the polarization energy is considered alone, the strong confinement regime is no longer valid, because $\sigma \leqslant 0$. For $R \lesssim 30$ Å, Fig. 2 shows that the Stark shift, computed up to the zeroth order, is underestimated. The results become much more accurate, when first order terms are included, and seem efficient enough for describing QCSE in spherical semiconductor QDs. As soon as $R \gtrsim 30$ Å, our results diverge from experimental data, as expected. When Coulomb interaction and polarization energy are included in the strong confinement regime, the weak field limit is no longer valid for QD radii $30\ Å \lesssim R \lesssim 50$ Å. Thus, a future work may focus on conciliating strong confinement regime and strong field limit. The case of the weak confinement regime is much more difficult to study, even in the weak field limit.

Table 1
Comparison of $\eta(\lambda)$ values from computational results of [8] and theoretical results given by equation $\eta(\lambda) = 0.208\frac{(1+\lambda)^2}{\lambda}$.

λ	1	3	5
$\eta_{comp}(\lambda)$	0.73	1.1	1.4
$\eta_{theo}(\lambda)$	0.83	1.1	1.5
Relative error (%)	≈14	<1	≈7

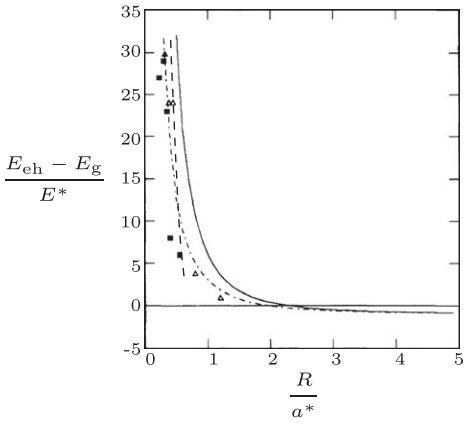

Fig. 1. Electron–hole pair ground state energy as a function of the QD radius computed for a confining infinite potential well with (—·-) or without (—) the presence of the pseudo-potential $W(\mathbf{r}_{e,h})$ and for a confining finite potential step of height $V_0 \approx 1$eV (-··-) [20] and compared to experimental results for *CdS* microcrystallites [21].

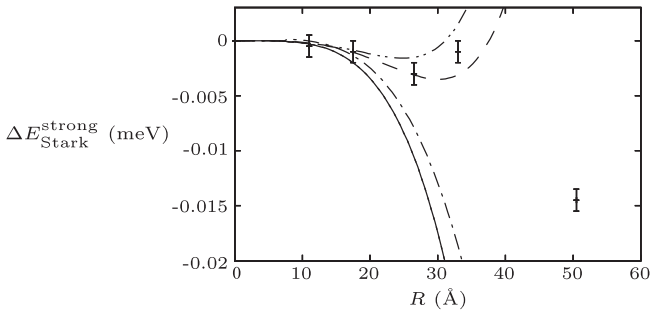

Fig. 2. Stark shift for electron–hole pair as a function of the QD radius, when $E_d = 12.5 kV.cm^{-1}$, only including the Coulomb interaction ($\Gamma_{eh} \approx -0.163$) up to the zeroth (—) or to the first (-·-) order, only including the polarization energy ($\Gamma_{eh} \approx -0.042$) up to the first order (-··-), and including both the Coulomb interaction and the polarization energy ($\Gamma_{eh} \approx -0.205$) up to the first order (-···-), in comparison with results (+) from [9].

4. Lamb shift

The Lamb effect comes from the effect of a quantized electromagnetic field on the motion of a quantum particle of mass m^* and charge qe in a potential $U(\mathbf{r})$. Two popular methods to compute

[1] $W(\mathbf{r}_{eh})$ should be attractive at distances $\approx a^*$ to promote excitonic state with typical size around a^*, repulsive at short distances to penalize small size excitonic states, and exponentially small at large distances.